CHEMISTRY
AN ASIAN JOURNAL
www.chemasianj.org

Accepted Article

Title: Hypoxia Activated Prodrugs of PERK Inhibitors

Authors: Lydia P. Liew, Dean C. Singleton, Way W. Wong, Gary J. Cheng, Stephen M.F. Jamieson, and Michael Hay

To be cited as: *Chem. Asian J.* 10.1002/asia.201801826

Link to VoR: http://dx.doi.org/10.1002/asia.201801826

A Journal of
ACES Asian Chemical Editorial Society

A sister journal of Angewandte Chemie and Chemistry – A European Journal

WILEY-VCH

10.1002/asia.201801826

WILEY-VCH

FULL PAPER

Hypoxia Activated Prodrugs of PERK Inhibitors

Lydia P. Liew [a,b], Dean C. Singleton [a,b], Way W. Wong [a], Gary J. Cheng [a], Stephen M.F. Jamieson [a,b,c] and Michael P. Hay* [a,b]

[a] Dr L.P. Liew (0000-0002-9322-2010), Dr D.C. Singleton (0000-0002-2044-8078), Ms W.W. Wong, Mr G.J. Cheng (0000-0002-2700-2415), Dr S.M.F. Jamieson (0000-0002-5485-9211), Assoc. Prof. M.P. Hay *(0000-0002-7087-9087)
Auckland Cancer Society Research Centre,
School of Medical Sciences,
Faculty of Medical and Health Sciences,
University of Auckland,
Private Bag 92019,
Auckland, New Zealand
E-mail: m.hay@auckland.ac.nz

[b] Dr L.P. Liew, Dr D.C. Singleton, Dr S.M.F. Jamieson, Assoc. Prof. M.P. Hay
Maurice Wilkins Centre for Molecular Biodiscovery
University of Auckland
Symonds St
Auckland 1010 New Zealand

[c] Dr S.M.F. Jamieson,
Department of Pharmacology and Clinical Pharmacology,
School of Medical Sciences,
Faculty of Medical and Health Sciences,
University of Auckland,
Private Bag 92019,
Auckland, New Zealand

Supporting information for this article is given via a link at the end of the document.

Abstract: Tumour hypoxia plays an important role in tumour progression and resistance to therapy. Under hypoxia unfolded proteins accumulate in the endoplasmic reticulum (ER) and this stress is relieved through the protein kinase R-like ER kinase (PERK) signalling arm of the unfolded protein response (UPR). Targeting the UPR through PERK kinase inhibitors provides tumour growth inhibition, but also elicits on-mechanism normal tissue toxicity. Hypoxia presents a target for tumour-selective drug delivery using hypoxia-activated prodrugs. We designed and prepared hypoxia-activated prodrugs of modified PERK inhibitors using a 2-nitromidazole bioreductive trigger. The new inhibitors retained PERK kinase inhibitory activity and the corresponding prodrugs were strongly deactivated. The prodrugs were able to undergo fragmentation following radiolytic reduction, or bioreduction in HCT116 cells, to release their effectors, albeit inefficiently. We examined the effects of the prodrugs on PERK signalling in hypoxic HCT116 cells. This study has identified a 2-substituted nitroimidazole carbamate prodrug with potential to deliver PERK inhibitors in a hypoxia selective manner.

Introduction

The endoplasmic reticulum (ER) provides an appropriate environment for the synthesis and maturation of proteins. Within the ER, protein folding occurs co-translationally, as well as post-translationally, through the introduction of disulphide bonds by the protein disulphide isomerase (PDI).[1] PDI participates in a redox relay with ER oxidases, requiring a terminal electron acceptor to support disulphide bond formation. While the role of oxygen as the terminal electron acceptor in cells is unclear, the post-translational folding of protein is oxygen-dependent.[1] Under hypoxic conditions, unfolded proteins accumulate in the ER, producing ER stress and activation of the unfolded protein response (UPR).[1] Consequently, the UPR can be considered as one of the key oxygen sensors, along with the hypoxia-inducible factors (HIF), which mediate adaptation to hypoxia.[2]

The UPR mediates both pro-survival and pro-apoptotic cellular responses. Accumulation of unfolded proteins activates three different sensors located in the lumen of the ER, protein kinase R (PKR)-like endoplasmic reticulum kinase (PERK/EIF2AK3), inositol-requiring protein α (IRE1α) and activating transcription factor-6 (ATF6), which control downstream signal transduction pathways to regulate ER stress.[3] The UPR acts to lower protein synthesis and reduce nascent protein translocation to the ER to manage protein load in the short term. The UPR also upregulates expression of chaperones involved in protein folding and degradative pathways to provide longer-term relief from ER stress.[2,4] Following these initial adaptive responses, the later stages of the UPR seek to restore basal levels of protein synthesis.[5] If ER stress remains unresolved this phase of the UPR produces excessive levels of oxidative stress resulting in the induction of cell death.

In the context of cancer, the activated UPR supports the growth and survival of tumour cells within a hostile environment.[6] Tolerance to hypoxia-induced ER stress is mediated primarily through the PERK pathway.[7] PERK activation occurs when the chaperone GRP78 dissociates from the luminal domain of the protein, allowing PERK to oligomerise and autophosphorylate.[8,9] Subsequent phosphorylation of Ser51 on cytoplasmic eukaryotic initiation factor 2α (eIF2α) promotes preferential translation of the transcription factor ATF4. ATF4 induces the transcription of chaperones, antioxidants and autophagy promoting genes.[10] Inhibitors of PERK phosphorylation of eIF2α have been developed.[11-13] For example, GSK2606414 (**1**) (IC_{50} = 0.4 nM) is

10.1002/asia.201801826

a first-in-class PERK inhibitor and its analogue GSK2656157 (**2**) (IC_{50} = 0.8 nM) was subsequently developed as a preclinical candidate.[11,14] Crystal structures of PERK with **1** and **2** bound show both inhibitors binding similarly (Figure 1).[11,12] The amino-pyrimidine motif anchors the inhibitors to the hinge binding region, while the central indoline core orientates the aryl acetamide to a lipophilic back pocket in the ATP binding site.[11,12] The specificity of these inhibitors for the PERK receptor is reliant on interactions with this hydrophobic back pocket.[11] As potent PERK inhibitors, both **1** and **2** were shown to inhibit tumour growth in pancreatic and myeloma xenograft models.[11,14]

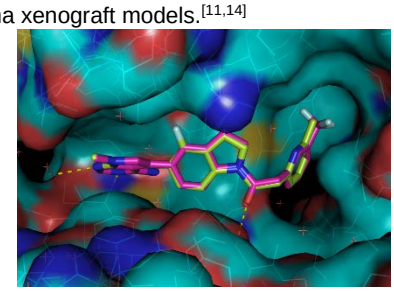

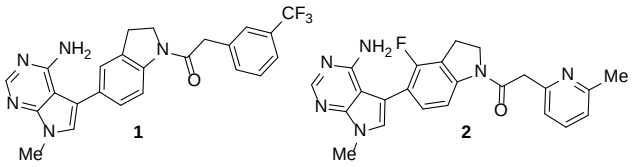

Figure 1. PERK inhibitors **1** (pink sticks) and **2** (green sticks) adopt a similar orientation in the ATP binding site. The activation loop (DFG motif) obscuring the binding site has been removed for clarity. Image produced in PyMOL v 1.7.0.1 (pdb 4G31 and 4M7I).[11,12]

While PERK is an attractive target for drug development, its well-defined role in the function of specialised secretory cells raises the spectre that UPR inhibition may be toxic to normal pancreas, liver and immune cells.[15,16] Indeed, treatment of tumour-bearing mice with **2** "caused damage to exocrine cells as well as pancreatic β-cells. These effects were also observed in rats and dogs treated with GSK2656157",[14] thus precluding further development. Nonetheless, the evidence that PERK acts as a survival factor under hypoxia[7,17,18], and mediates metastasis[19,20] provides a clear argument for the selective delivery of PERK inhibitors to hypoxic areas of tumours. This would be expected to maximise drug delivery to tumour cells that are dependent on PERK signalling for survival, while minimizing normal tissue drug exposure, and thus providing an improved therapeutic index.

Hypoxia is a cardinal element of the tumour microenvironment and plays a major role in tumour progression and response to treatment.[21] Hypoxic cells also contribute to resistance to therapy.[22-24] Nonetheless, hypoxia provides a tumour-specific address for drug delivery.[25,26] Hypoxia-activated prodrugs (HAPs) are enzymatically reduced in hypoxic tissue to release active drugs which may diffuse to adjacent tumour tissue (a molecular "bystander effect").[25-28] While early work focussed on delivering DNA-reactive cytotoxins such as PR104,[29] SN30000[30,31] and TH-302 (evofosfamide),[32] there is growing interest in using HAPs to deliver molecularly targeted agents.[33-35] We have explored various prodrug chemistries to deliver drugs to hypoxic tumour cells[36-40] and, along with others,[41-44] have identified 2-nitroimidazole methyl ethers and carbamates as useful "triggers" for HAPs that fragment when reduced (Scheme 1).[45-47] One-electron reductases, such as cytochrome P450 oxidoreductase (POR),[48] reduce 2-nitroimidazoles to a nitro radical anion which readily reacts with oxygen in a futile cycle. In the absence of oxygen further reduction leads to the hydroxylamine (and amine) which fragment to release a reactive iminium cation and the corresponding phenol. In the case of carbamates, a carbamic acid is released which readily fragments to the amine. In this work we exemplify a HAP approach to deliver PERK inhibitors to hypoxic cells.

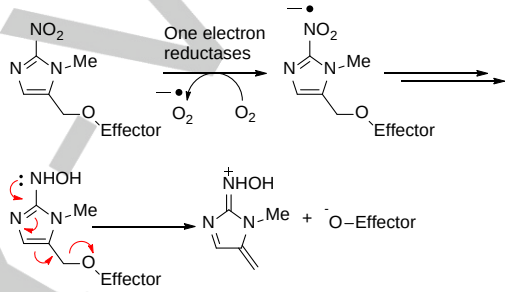

Scheme 1. Mechanism of bioreductive activation of 2-nitroimidazole prodrugs.

Results and Discussion

Design and synthesis of PERK inhibitors and prodrugs

The lipophilic pocket occupied by the 3-methylpyridyl group (Figure 1) was identified as providing specificity for PERK and presented an opportunity to design prodrugs where addition of significant steric bulk would reduce PERK kinase activity. Our starting point was to prepare a series of methoxy-substituted inhibitors **3**–**5** based on the known inhibitor **4** (IC_{50} = 0.5 nM) (Figure 2).[11] We designed a series of phenols **6a**–**8a** as potential PERK inhibitors (effectors), which could be released from the corresponding 2-nitroimidazole methyl ether HAPs (**6b**–**8b**) after bioreduction.

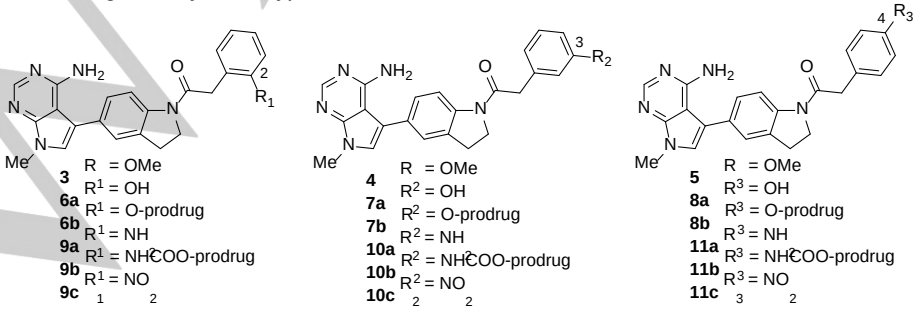

Figure 2. PERK inhibitors and prodrugs.

10.1002/asia.201801826

We also considered a series of anilines **9a**–**11a** where the prodrugs (**9b**–**11b**) are linked by a carbamate moiety.

The indoline coupling partner **12** was obtained in seven steps from 4-chloropyrimidine and 5-bromoindoline using a known, convergent synthetic route with minor modifications.[11] The PERK inhibitors (**3**–**5**, **6a**–**8a**) were prepared by coupling indoline **12** with the appropriate phenylacetic acids using HATU or EDCl in variable yields (Scheme 2). We observed that portion wise addition of the acid or HATU to the reaction mixture resulted in improved yields. Pre-treatment of phenylacetic acids with HATU appears to form a stable intermediate species, which could not be displaced by the indoline **12**. This is consistent with the *m/z* ion corresponding to an activated ester detected by LRMS when the reaction was terminated.

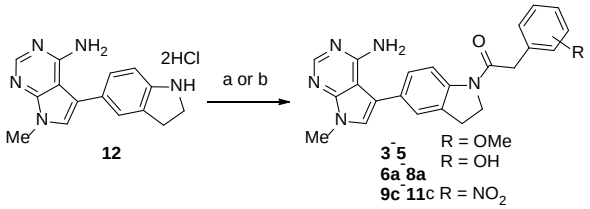

Scheme 2. Amide coupling. Reaction conditions. a) HATU, DIPEA, DMF, overnight, 23–90%; b) EDCl, DIPEA, DMAP, CH_2Cl_2, overnight, 41–80%.

We envisioned that the aniline targets **9a**–**11a** would be obtained by coupling the nitro-substituted phenylacetic acids to indoline **12** followed by reduction. The nitro compounds **9c**–**11c** were prepared using HATU as a coupling agent (Scheme 2). We were able to prepare **9a** using zinc reduction in 72% yield, but met with difficulties in reducing **10c**. We attempted reduction of **10c** with $SnCl_2$ and hydrogenation conditions (H_2 at 40 psi, 10% Pd/C), but the substrate **10c** was poorly soluble in the solvents used. We turned to a longer preparation, requiring an additional BOC-protection step (Scheme 3). The phenylacetic acids **13** and **14** were coupled to **12** with HATU to give amides **15** and **16**, respectively. Removal of the protecting group with TFA provided anilines **10a** and **11a** in 73 and 76% over 3 steps, respectively.

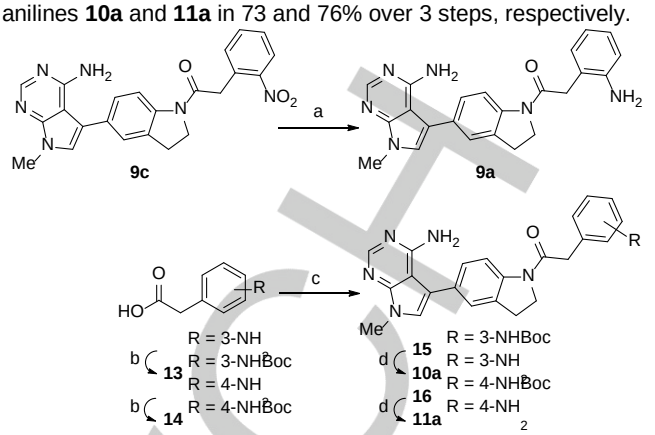

Scheme 3. Synthesis of aniline targets **9a**–**11a**. Reaction conditions. a) Zn dust, NH_4Cl, DMF/acetone/water (3:3:2), 3 h, 72%; b) di-*tert*-butyl-dicarbonate, 1M NaOH, dioxane/water (2:1), 24 h, 90–91%; c) **12**, HATU, DIPEA, DMF, overnight, 88–93% d) TFA, DCM, 4–5 h, 86–96%.

With the effectors in hand, we turned our attention to the synthesis of the prodrugs. The bioreductive trigger 2-nitroimidazole-5-methanol (**17**) was prepared according to literature procedure.[34] Alcohol **17** was converted to the chloride **18** with MsCl (Scheme 4). Alkylation of phenols **6a**-**8a** gave the ether prodrugs **6b**–**8b**, respectively. In all examples, the reaction did not proceed to completion, even with heating to 70 °C over 3 days in the case of **6b**. A side-product in the crude reaction mixture with a structure corresponding the formyl imidazole (See Figure **S1**) was observed in the crude reaction mixtures in all cases, which necessitated purification by preparative HPLC. The alcohol **17** was activated as the 4-nitrophenylcarbonate **19**,[46] and reaction with amines **9a–11a** gave carbamate prodrugs **9b-11b** in modest yields.

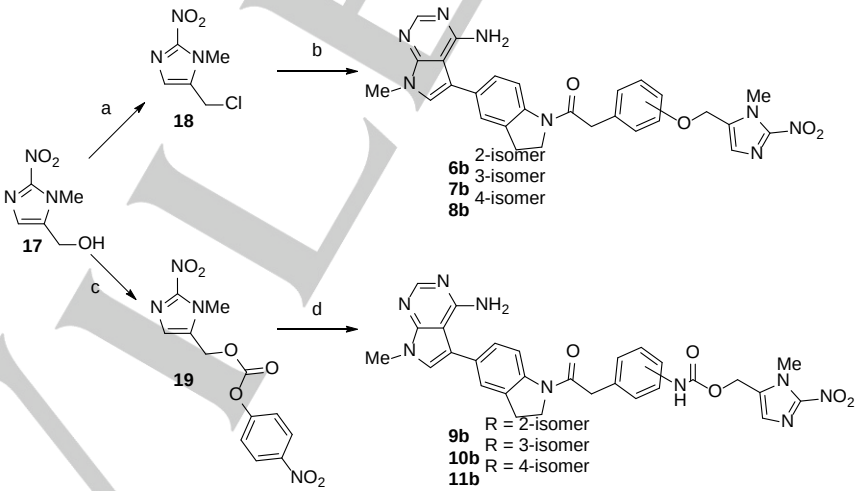

Scheme 4. Prodrug formation. Reaction conditions. (a) MsCl, DIPEA, THF, 30 min, 99%; (b) Phenol (**6a**–**8a**), KI, K_2CO_3, DMF, 28–32%; (c) nitrophenyl chloroformate, DIPEA, THF, 16 h, 25%; (d) anilines (**9a**–**11a**), DIPEA, HOBt, 5 Å molecular sieves, THF, 72 h, 9–58%.

Inhibition of PERK activity

The biochemical potency of the inhibitors and prodrugs against PERK was determined for human EIF2AK3 phosphorylation of myelin basic protein (10 μM) with ^{33}P-ATP (10 μM). Ten point titration curves were determined in duplicate and an IC_{50} calculated. (Reaction Biology Corp, Malvern, PA) (Table 1). The new inhibitors were found to have retained substantial inhibitory activity (IC_{50} 1.2–60.7 nM) against PERK, while the prodrugs demonstrated a considerable loss of potency. Inhibitors with a

para-substituent were found to be less active (~10-fold) than their corresponding *ortho*- or *meta*-substituted analogues, again consistent with previous reports.[11] The ether prodrugs **6b**–**8b** demonstrated >100-fold deactivation as PERK inhibitors, while the carbamate prodrugs **9b**–**11b** demonstrated >1000-fold deactivation compared to **9a**–**11a**. The potency of the PERK inhibitors was independent of the electronic or hydrogen bonding nature of the substituents and was mostly influenced by the size of the substituent, consistent with a steric interaction with the pocket. Substitution at the 4-position was least favoured across the series and this is consistent with previous findings.[11]

Table 1. Biochemical IC_{50} values for PERK inhibitors and prodrugs.

Compound	R Group	PERK/EIF2AK3 IC50 (nM)[a]	Selectivity ratios
1 (GSK'414)	3-CF_3	1.6	
3	2-OMe	1.4	
4	3-OMe	1.5	
5	4-OMe	20.7	
6a	2-OH	16.3	
7a	3-OH	11.1	
8a	4-OH	26.0	
6b	2-*O*-prodrug	2080	128
7b	3-*O*-prodrug	1570	141
8b	4-*O*-prodrug	84000	3231
9a	2-NH_2	1.2	
10a	3-NH_2	3.2	
11a	4-NH_2	60.7	
9b	2-*NHCOO*-prodrug	1619	1349
10b	3-*NHCOO*-prodrug	27820	8694
11b	4-*NHCOO*-prodrug	101335	1669
9c	2-NO_2	41.1	
10c	3-NO_2	1.4	
11c	4-NO_2	26.5	

[a] IC_{50} determinations were performed by Reaction Biology Corp.

Prodrug fragmentation

Reduction of prodrugs and subsequent release of the corresponding PERK inhibitors was measured following radiolytic reduction (40 Gy) of anoxic solutions of prodrugs in formate buffer with subsequent analysis by LC-MS.[37] Strongly reducing species (aquated electron, $e^-(aq)$ and formate radical, $CO_2^{\cdot-}$) are produced by radiolysis which result in reduction of the nitroimidazole group. In all six examples, the prodrugs underwent fragmentation to release the effector, albeit somewhat inefficiently. In the ether series, the *ortho*-substituted compound **6b** exhibited the greatest loss of prodrug, followed by *meta*-and *para*- substituted analogues, **7b** and **8b**, respectively. This order is reversed for the carbamate series of prodrugs, with the *para*-substituted prodrug **11b** showing the greatest fragmentation and followed by the *meta*- and *ortho*-substituted prodrugs **10b** and **9b**, respectively. The rates of reduction appear to be slower in the prodrugs containing an ether linkage (38–58%) and in **9b**, whereas the carbamate prodrugs **10b** and **11b** demonstrated greater loss of prodrug.

The 2-substituted carbamate prodrug **9b** was able to achieve the most effective prodrug to effector conversion, with a G_{gain} to G_{loss} ratio of approximately 50%. All other examples suggest that while the prodrugs are able to undergo fragmentation to release its effector, the conversion to effector is inefficient and will require further optimisation.

Table 2. Rates of prodrug fragmentation

#	Prodrug	% Loss of prodrug	G_{loss} [a] (μM/Gy)	G_{gain} [b] (μM/Gy)
6b	2-*O*-	58	0.146	0.007
7b	3-*O*-	43	0.108	0.016
8b	4-*O*-	38	0.047	0.009
9b	2-*NHCO₂*-	27 ± 7[c]	0.07 ± 0.02	0.035 ± 0.003
10b	3-*NHCO₂*-	84 ± 5	0.21 ± 0.01	0.056 ± 0.001
11b	4-*NHCO₂*-	93 ± 1	0.233 ± 0.002	0.026 ± 0.0002

[a] G_{loss} measures the loss of prodrug. [b] G_{gain} measures the effector being released. [c] Values ± SEM.

Target modulation of the UPR

We used HCT116 colorectal carcinoma cells to investigate the ability of the PERK HAPs and their corresponding effectors to modulate anoxia-induced PERK signalling. Four prodrug/effector pairs were selected for this study, excluding the *para*-substituted analogues **8a**,**b** because of the poor aqueous stability of **8b** (7% over 24 h) and **11a**,**b** because the low aqueous solubility of **11b** (Table S1). Three of the prodrugs (**6b**, **7b**, **9b**) and all four effectors (**6a**, **7a**, **9a**, **10a**) were stable, both in cell-free culture medium incubated for 24 h at 37°C in oxic conditions, or in the presence of HCT116 cells cultured for 24 h either in oxic conditions (Figure S3). Loss of prodrug **10b** was observed in both the oxic and anoxic cell culture, but not in cell-free conditions, suggesting cellular metabolism. Notably, anoxic prodrug activation and release was observed with **6b**, **7b**, **9b** and **10b**, generated effector concentrations of 0.27, 0.82, 0.27, and 1.2 μM, respectively, in the extracellular culture medium after 24 h anoxic exposure (Figure 3A). In contrast, none of the four prodrugs generated effector species in oxic HCT116 cultures, confirming the predicted oxygen-sensitive mechanism of prodrug activation. We confirmed the hypoxia-selective activation and effector

10.1002/asia.201801826

release for **7b** using HCT116 POR-overexpressing cells (Figure S5, 4h drug exposure).

DDIT3 (CHOP) and *PPP1R15A* (GADD34) are well-validated, downstream transcriptional targets of ATF4 and, thus, act as sensitive biomarkers of PERK-eIF2α-ATF4 pathway activity. *DDIT3* transcript, assessed by RT-qPCR, was up-regulated by 24.7- to 29.7-fold in HCT116 cells following 24 h anoxic exposure, confirming anoxia-induced ER stress resulting in PERK activation (Figure 3B). Of the PERK inhibitors tested, **7a**, **9a** and **10a** all suppressed anoxic up-regulation of *DDIT3* by 6.3-, 10.2- and 11.2-fold, respectively. **6a** was inactive. Paradoxically, the inhibitors all induced *DDIT3* expression in normoxic (unstressed) cultures by 4.3- to 10.7-fold, suggesting activation of ATF4, at least with exposure to 10 μM compound. Both **7b** and **9b** demonstrated suppression of anoxic *DDIT3* up-regulation to 17.4- and 6.0–fold, respectively, consistent with the observed effector released in these conditions (Figure 3A). **6b** and **10b** did not suppress anoxic *DDIT3* up-regulation despite similar levels of effector generated during anoxic exposure. Under oxic conditions neither **7b** nor **9b** activated PERK signalling in keeping with the lack of effector generated in oxic cultures.

PPP1R15A expression was modestly induced under anoxic conditions. Suppression of anoxic *PPP1R15A* (GADD34) expression was observed (2.9- to 5.1–fold) with all effectors and with one prodrug (**9b**), in agreement with the effects observed *DDIT3*. All effectors suppressed anoxic *PPP1R15A* up-regulation (to 0.69- to 1.4-fold) and appeared to modestly activate expression under oxic conditions (by 1.3- to 2.5-fold). Of the prodrugs, only **9b** was effective in suppressing anoxic-induced expression. **6b** was inactive and **7b** and **10b** caused an unexpected up-regulation of *PPP1R15A* expression in anoxic conditions, possibly due to activation of apoptosis as evidenced by an induction of PARP1 cleavage (data not shown).

Western immunoblotting was conducted with the same prodrug/effector pairs. Both ATF4 and CHOP protein levels were induced following treatment with anoxic ER stress, confirming activation of the PERK-eIF2α-ATF4 branch of the UPR (Figure 3C). All effectors suppressed the up-regulation of CHOP expression in response to anoxia, however, effects on ATF4 were not observed. ATF4, and to a lesser extent CHOP, were also induced in oxic cultures treated with each effector, and also with prodrugs **6b** and **7b**, in agreement with the RT-qPCR analysis. Two of the prodrugs (**7b** and **9b**) suppressed anoxic CHOP up-regulation, with minor effect on ATF4 and minimal effects in oxic cultures with **9b** showing marginal superiority. Prodrugs **6b** and **10b** were inactive. Overall, **9b** appeared to be the best prodrug demonstrating the greatest magnitude of PERK-eIF2α-ATF4 inhibition under anoxia with negligible effects on the pathway under oxic conditions.

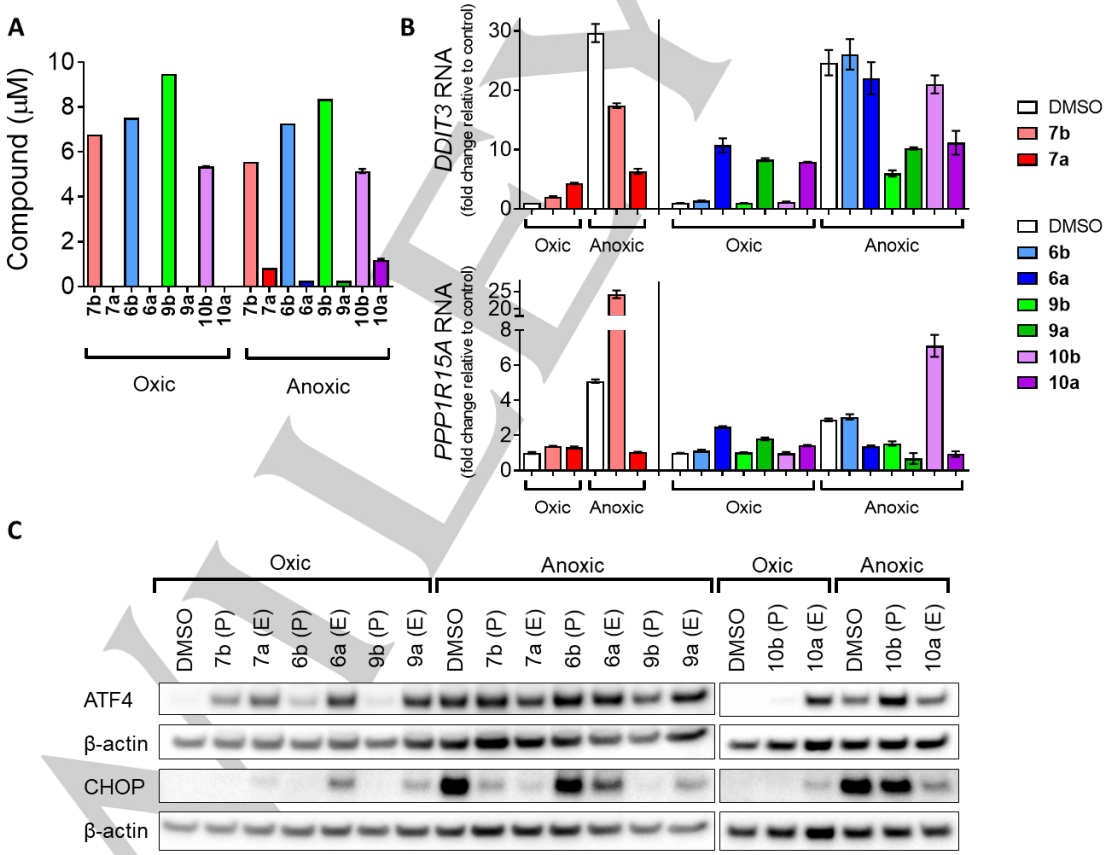

Figure 3. Evaluation of hypoxia-activated PERK inhibitor prodrugs and effectors in HCT116 cells. A. Concentrations of prodrugs and effectors in HCT116 culture medium. HCT116 cultures were treated with 10 μM prodrug for 24 h in oxic or anoxic conditions (mean ± SD, n = 1-2). B. Effect of 10 μM PERK prodrug/effector on DDIT3 and PPP1R15A transcript abundance in HCT116 cells cultured for 24 h in oxic or anoxic conditions (mean ± SEM, n = 2-3). C. Effect of 10 μM PERK prodrug/effector pairs on ATF4 and CHOP protein abundance in HCT116 cells cultured for 24 h in oxic or anoxic conditions.

Conclusions

We adapted a known class of PERK inhibitor and prepared new analogues with phenol or aniline linkers and the corresponding ether and carbamate hypoxia-activated prodrugs. The modified inhibitors retained PERK inhibitory activity and the corresponding prodrugs were substantial deactivated. We demonstrated the prodrugs were able to undergo fragmentation following radiolytic reduction to release their effectors, albeit inefficiently. The prodrugs also underwent bioreduction in HCT116 cells under anoxic conditions releasing effector, but not under oxic conditions, demonstrating hypoxia-dependent fragmentation of the 2-nitroimidazole trigger. However, the relatively high concentration of both effectors and prodrugs did cause unexpected effects, especially on ATF4 abundance and likely on cell survival. While this class has been described as particularly selective for PERK, analogues did engage with a variety of kinases at 10 μM.[11,12] Subsequent work has also identified RIPK1 kinase as a target kinase for compound **1**.[49] Given these observations, it seems plausible that the high concentrations of effectors and prodrugs used in our cellular studies may have induced off-target effects. Nonetheless, this study has identified the 2-substituted nitroimidazole carbamate **9b** as a prodrug with potential to deliver PERK inhibitors in a hypoxia selective manner. Key steps to further development is to increase aqueous solubility, enhance the rates of fragmentation and gain a broader understanding of the off-target effects of these compounds.

Experimental Section

Chemistry Synthesis

General procedures. All final products were analysed by reverse-phase HPLC, (ZORBAX Eclipse XDB C8 5 μm column, 4.6 × 150 mm; Agilent Technologies or an Altima C18 5μm column, 3.2 × 150 mm) using an Agilent Technologies 1260 Infinity equipped with a diode-array detector. Mobile phases were gradients of 80% acetonitrile/20% H_2O (v/v) in 45 mM ammonium formate at pH 3.5 and 0.7-1.2 mL/min. Final compound purity was determined by monitoring at 330 ± 50 nM and was >95%, with the exception of **8b** (93.9%). Melting points were determined on an Electrothermal 2300 Melting Point Apparatus. NMR spectra were obtained on a Bruker Avance 400 spectrometer at 400 MHz for ^{1}H and 100 MHz for ^{13}C spectra. Spectra were obtained in DMSO-d_6 unless noted otherwise. Chemical shifts and coupling constants were recorded in units of ppm and Hz, respectively. Low resolution mass spectra were gathered by direct injection of methanolic solutions into an Agilent 6120 mass spectrometer using an atmospheric pressure chemical ionization (APCI) mode with a fragmentor voltage of 50 V and a drying gas temperature of 250 °C. High resolution mass spectra (HRMS) were measured on an Agilent Technologies 6530 Accurate-Mass Quadrupole Time of Flight (Q-TOF) LC / MS interfaced with an Agilent Jet Stream Electrospray Ionization (ESI) source allowing positive or negative ions detection. Organic solutions were dried over Na_2SO_4 and solvents were evaporated under reduced pressure on a rotary evaporator. Thin-layer chromatography was carried out on aluminium-backed silica gel plates (Merck 60 F_{254}) with visualization of components by UV light (254 nm) or exposure to I_2. Column chromatography was carried out on silica gel (Merck 230–400 mesh). CH_2Cl_2 refers to dichloromethane, DIPEA refers to diisopropylethylamine, DMAP refers to 4-dimethylaminopyridine, DMF refers to dimethylformamide, DMSO dimethyl sulfoxide, EDCI refers to 1-ethyl-3-(dimethylaminopropyl)carbodiimide, EtOAc refers to ethyl acetate, HATU refers to 2-(7-aza-1H-benzotriazole-1-yl)-1,1,3,3-tetramethyluronium hexafluorophosphate, MeOH refers to methanol, pet. ether refers to petroleum ether boiling fraction 40–60 °C, THF refers to tetrahydrofuran, TFA refers to trifluoroacetic acid.

Amide coupling

Method A: HATU-mediated amide coupling

1-(5-(4-Amino-7-methyl-7*H*-pyrrolo[2,3-*d*]pyrimidin-5-yl)indolin-1-yl)-2-(2-methoxyphenyl)ethan-1-one (3). 2-Methoxyphenylacetic acid (49 mg, 0.30 mmol) was added portion wise to a stirred solution of amine **12** (100 mg, 0.30 mmol), HATU (112 mg, 0.30 mmol) and DIPEA (207 μL, 1.18 mmol) in DMF (5 mL). The reaction mixture was stirred at 20 °C for 24 h. The resulting mixture was diluted with EtOAc (50 mL), washed with water (2 × 50 mL) and then brine (50 mL), dried and concentrated *in vacuo*. The crude residue was purified by trituration with EtOAc to give amide **3** (110 mg, 90 %) as an off-white solid: m.p. 185–187°C; ^{1}H NMR: δ=8.14 (s, 1H, H-2), 8.10 (d, *J* = 8.3 Hz, 1H, H-7'), 7.30 (s, 1H, H-4'), 7.28–7.18 (m, 4H, H-6, H-6', H-4'', H-6''), 7.00 (d, *J* = 7.7 Hz, 1H, H-3''), 6.91 (td, *J* = 7.4, 1.0 Hz, 1H, H-5''), 6.06 (br s, 2H, NH_2-4), 4.22 (t, *J* = 8.4 Hz, 2H, H_2-2'), 3.77 (s, 5H, CH_2, OCH_3-2''), 3.72 (s, 3H, NCH_3-7), 3.23 ppm (t, *J* = 8.4 Hz, 2H, H_2-3'); ^{13}C NMR: δ=168.9 (C=O), 157.2 (C-2''), 157.1 (C-4), 151.6 (C-2), 150.3 (C-7a), 141.9 (C-7'a), 132.8 (C-3'a), 130.8 (C-6''), 129.7 (C-5'), 128.1 (C-4''), 127.1 (C-6'), 124.9 (C-4'), 123.9 (C-6), 123.7 (C-1''), 120.2 (C-5''), 116.1 (C-7'), 115.0 (C-5), 110.7 (C-3''), 99.9 (C-4a), 55.4 (OCH_3-2''), 47.9 (C-2'), 36.7 (CH_2), 30.7 (NCH_3-7), 27.5 ppm (C-3'); MS (APCI): *m/z* (%): 414.2 (100) $[M+H]^+$; HRMS (ESI): *m/z* calcd for $C_{24}H_{24}N_5O_2$: 414.1925 $[M+H]^+$; found: 414.1933; HPLC purity: 98.2 %.

Method B: EDCI-mediated amide coupling

1-(5-(4-Amino-7-methyl-7*H*-pyrrolo[2,3-*d*]pyrimidin-5-yl)indolin-1-yl)-2-(3-methoxyphenyl)ethan-1-one (4). EDCI (116 mg, 0.60 mmol) was added to a stirred solution of 3-methoxyphenylacetic acid (100 mg, 0.60 mmol) and DIPEA (420 μL, 2.41 mmol) in CH_2Cl_2 (5 mL) and stirred for 5 min. DMAP (74 mg, 0.60 mmol) and 5-(indolin-4-yl)-7-methyl-7*H*-pyrrolo[2,3-*d*]pyrimidin-4-amine (**12**) (160 mg, 0.47 mmol), which have been prepared according to literature procedure was added to the mixture.[12] The reaction mixture was stirred at 20 °C for 24 and diluted with CH_2Cl_2 (50 mL). The organic layer was washed with water (50 mL) and with brine (50 mL), dried and concentrated to give amide **4** (157 mg, 80 %) as a white solid: m.p. 230–233°C; ^{1}H NMR: δ=8.14–8.12 (m, 2H, H-2, H-7'), 7.29 (s, 1H, H-4'), 7.27–7.21 (m, 3H, H-6, H-6', H-5''), 6.88–6.87 (m, 2H, H-2'', H-6''), 6.83 (dd, *J* = 8.2, 2.4 Hz, 1H, H-4''), 6.05 (br s, 2H, NH_2-4), 4.19 (t, *J* = 8.4 Hz, 2H, H_2-2'), 3.83 (s, 2H, CH_2), 3.75 (s, 3H, OCH_3-3''), 3.72 (s, 3H, NCH_3, 3.20 ppm (t, *J* = 8.4 Hz, 2H, H_2-3'); ^{13}C NMR: δ=168.9 (C=O), 159.2 (C-3''), 157.1 (C-3''), 151.6 (C-2), 150.3 (C-

7a), 141.8 (C-7'a), 136.5 (C-1''), 132.8 (C-3'a), 129.8 (C-5'), 129.3 (C-5''), 127.1 (C-6'), 124.9 (C-4'), 124.0 (C-6), 121.6 (C-6''), 116.2 (C-7'), 115.2 (C-2''), 114.9 (C-5), 111.9 (C-4''), 99.8 (C-4a), 55.0 (OCH_3-3''), 47.9 (C-2'), 42.1 (CH_2), 30.7 (N-Me), 27.5 ppm (C-3'); MS (APCI): *m/z* (%): 414.2 (100) $[M+H]^+$; HRMS (ESI): *m/z* calcd for $C_{24}H_{24}N_5O_2$: 414.1925 $[M+H]^+$; found: 414.1917; HPLC purity: 99.3 %. ^{1}H NMR data was found to be consistent with literature.[11]

1-(5-(4-Amino-7-methyl-7*H*-pyrrolo[2,3-*d*]pyrimidin-5-yl)indolin-1-yl)-2-(4-methoxyphenyl)ethan-1-one (5). Prepared using method B. The resulting residue was diluted in EtOAc and washed with 0.4M HCl to obtain **5** as the HCl salt (41 %) as a white solid: m.p. 186–189°C; ^{1}H NMR: δ=8.48 (s, 1H, H-2), 8.16 (d, *J* = 8.2 Hz, 1H, H-7'), 7.58 (s, 1H, H-6), 7.30 (s, 1H, H-4'), 7.25–7.21 (m, 3H, H-6', H-2'', H-6''), 6.90 (ddd, *J* = 8.7, 2.9, 2.0 Hz, 2H, H-3'', H-5''), 4.20 (t, *J* = 8.4 Hz, 2H, H_2-2'), 3.83 (s, 3H, N-Me), 3.80 (s, 2H, CH_2), 3.74 (s, 3H, OCH_3-4), 3.20 ppm (t, *J* = 8.4 Hz, 2H, H_2-3'), NH_2 not observed; ^{13}C NMR: δ=169.5 (C=O), 158.0 (C-4''), 151.3 (C-4), 147.5 (C-7a), 142.7 (C-2), 142.6 (C-7'a), 133.1 (C-3'a), 130.4 (C-3'', C-5''), 127.3 (C-5'), 127.2 (C-6'), 127.1 (C-6), 126.8 (C-1''), 124.8 (C-4'), 117.9 (C-5), 116.4 (C-7'), 113.8 (C-3'', C-5''), 98.4 (C-4a), 55.0 (OCH_3-4''), 47.9 (C-2'), 41.3 (CH_2), 31.5 (N-Me), 27.5 ppm (C-3'); MS (APCI): *m/z* (%): 414.2 (100) $[M+H]^+$; HRMS (ESI): *m/z* calcd for $C_{24}H_{24}N_5O_2$: 414.1925 $[M+H]^+$; found: 414.1940; HPLC purity: 99.0 %.

1-(5-(4-Amino-7-methyl-7*H*-pyrrolo[2,3-d]pyrimidin-5-yl)indolin-1-yl)-2-(2-hydroxyphenyl)ethan-1-one (6a). Prepared using method A and purified by column chromatography (5% MeOH/EtOAc) to afford **6a** (23 %) as an off-white white solid: m.p. 252–255°C; ^{1}H NMR: δ=9.47 (s, 1H, OH-2''), 8.15 (s, 1H, H-2), 8.12 (d, *J* = 8.3 Hz, 1H, H-7'), 7.30 (s, 1H, H-4'), 7.26 (s, 1H, H-6), 7.21 (dd, *J* = 8.3, 1.4 Hz, 1H, H-6'), 7.13–7.06 (m, 2H, H-4'', H-6''), 6.82 (dd, *J* = 8.1, 0.8 Hz, 1H, H-3''), 6.76 (td, *J* = 7.4, 0.9 Hz, 1H, H-5''), 6.13 (br s, 2H, NH_2), 4.22 (t, *J* = 8.4 Hz, 2H, H_2-2'), 3.74–3.73 (m, 5H, CH_2, Me), 3.21 ppm (t, *J* = 8.4 Hz, 2H, H_2-3'); ^{13}C NMR: δ=169.2 (C=O), 156.8 (C-4), 155.3 (C-2''), 151.1 (C-2), 150.2 (C-7a), 142.0 (C-7'a), 132.8 (C-3'a), 130.8 (C-6''), 129.5 (C-5'), 127.7 (C-4''), 127.1 (C-6'), 124.8 (C-4'), 124.1 (C-6), 121.8 (C-1''), 118.8 (C-5''), 116.1 (C-7'), 115.1 (C-5), 114.9 (C-3''), 99.8 (C-4a), 47.9 (C-2'), 36.7 (CH_2), 30.7 (Me), 27.5 ppm (C-3'); MS (APCI): *m/z* (%): 400.2 (100) $[M+H]^+$; HRMS (ESI): *m/z* calcd for $C_{23}H_{22}N_5O_2$: 400.1768 $[M+H]^+$; found: 400.1783; HPLC purity: 98.0 %.

1-(5-(4-Amino-7-methyl-7*H*-pyrrolo[2,3-d]pyrimidin-5-yl)indolin-1-yl)-2-(3-hydroxyphenyl)ethan-1-one (7a). Prepared using method A to obtain **7a** (28 %) as an off-white solid: m.p. 182–185°C; ^{1}H NMR: δ=9.39 (br s, 1H, OH-3''), 8.14–8.13 (m, 2H, H-2, H-7'), 7.28 (s, 1H, H-4'), 7.23–7.21 (m, 2H, H-6, H-6'), 7.14–7.10 (m, 1H, H-5''), 6.73–6.71 (m, 2H, H-2'', 6''), 6.66–6.64 (m, 1H, H-4''), 6.04 (br s, 2H, NH_2-4), 4.16 (t, *J* = 8.4 Hz, 2H, CH_2-2'), 3.76 (s, 2H, CH_2), 3.72 (s, 3H, Me), 3.18 ppm (t, *J* = 8.4 Hz, 2H, CH_2-3'); ^{13}C NMR: δ=169.1 (C=O), 157.4 (C-4), 157.2 (C-3''), 151.6 (C-2), 150.4 (C-7a), 141.9 (C-7'a), 136.2 (C-1''), 132.8 (C-3a), 129.8 (C-5'), 129.3 (C-5''), 127.1 (C-6'), 124.9 (C-4'), 124.0 (C-6), 120.0 (C-6''), 116.2 (C-7'), 116.1 (C-2''), 115.0 (C-5), 113.6 (C-4''), 99.9 (C-4a), 48.0 (C-2'), 42.4 (CH_2), 30.7 (Me), 27.5 ppm (C-3'); MS (APCI): *m/z* (%): 400.2 (100) $[M+H]^+$; HRMS (ESI): *m/z* calcd for $C_{23}H_{22}N_5O_2$: 400.1768 $[M+H]^+$; found: 400.1760; HPLC purity: 96.6 %.

1-(5-(4-Amino-7-methyl-7*H*-pyrrolo[2,3-d]pyrimidin-5-yl)indolin-1-yl)-2-(4-hydroxyphenyl)ethan-1-one (8a). Prepared using method A to obtain **8a** (76 %) as an off-white solid: m.p. 240–243°C; ^{1}H NMR: δ=9.30 (br s, 1H, OH-4''), 8.14–8.12 (m, 2H, H-2, H-7'), 7.28 (s, 1H, H-4'), 7.23–7.20 (m, 2H, H-6, H-6'), 7.09 (d, *J* = 8.4 Hz, 2H, H-3'', H-5''), 6.72 (ddd, *J* = 8.4, 2.8, 1.9 Hz, 2H, H-2'', H-6''), 6.04 (br s, 2H, NH_2-4), 4.17 (t, *J* = 8.4 Hz, 2H, H_2-2'), 3.72 (s, 5H, N-Me, CH_2), 3.18 ppm (t, *J* = 8.4 Hz, 2H, H_2-3'); ^{13}C NMR: δ=169.5 (C=O), 157.2 (C-4), 156.0 (C-4''), 151.6 (C-2), 150.3 (C-7a), 141.9 (C-7'a), 132.8 (C-3'a), 130.3 (C-2'', C-6''), 129.7 (C-5'), 127.1 (C-6'), 125.0 (C-4'), 124.8 (C-1''), 124.0 (C-6), 116.2 (C-7'), 115.2 (C-3'', C-5''), 115.0 (C-5), 99.9 (C-4a), 47.9 (C-2'), 41.4 (CH_2), 30.7 (N-Me), 27.5 ppm (C-3'); MS (APCI): *m/z* (%): 400.2 (100) $[M+H]^+$; HRMS (ESI): *m/z* calcd for $C_{23}H_{22}N_5O_2$: 400.1768 $[M+H]^+$; found: 400.1777; HPLC purity: 97.3 %.

1-(5-(4-Amino-7-methyl-7*H*-pyrrolo[2,3-d]pyrimidin-5-yl)indolin-1-yl)-2-(2-nitrophenyl)ethan-1-one (9c). Prepared using method A to obtain **9c** (quant.) as a yellow solid: m.p. 231–233°C; ^{1}H NMR: δ=8.14 (s, 1H, H-2), 8.11 (dd, 1H, *J* = 8.1, 1.2 Hz, 1H, H-3''), 8.00 (d, *J* = 8.2 Hz, 1H, H-7'), 7.73 (td, *J* = 7.5, 1.2 Hz, 1H, H-5''), 7.61–7.55 (m, 2H, H-4'', H-6''), 7.33 (s, 1H, H-4'), 7.24 (s, 1H, H-6), 7.20 (d, *J* = 8.2 Hz, 1H, H-6'), 6.06 (br s, 2H, NH_2-4), 4.33–4.29 (m, 4H, CH_2, H_2-2'), 3.72 (s, 3H, Me), 3.29 ppm (t obscured, *J* = 8.8 Hz, 2H, H_2-3'); ^{13}C NMR: δ=167.8 (C=O), 157.6 (C-4), 152.1 (C-2), 150.8 (C-7a), 149.6 (C-2''), 142.1 (C-7'a), 134.2 (C-5''), 134.2 (C-6''), 133.2 (C-3'a), 131.3 (C-1''), 130.4 (C-5'), 128.9 (C-4''), 127.6 (C-6'), 125.4 (C-4'), 125.1 (C-3''), 124.5 (C-6), 116.5 (C-7'), 115.4 (C-5), 100.3 (C-4a), 48.3 (C-2'), 40.9 (CH_2), 31.2 (Me), 28.0 ppm (C-3'); MS (APCI): *m/z* (%): 429.2 (100) $[M+H]^+$; HRMS (ESI): *m/z* calcd for $C_{23}H_{21}N_6O_3$: 429.1670 $[M+H]^+$; found: 429.1690; HPLC purity: 99.4 %.

1-(5-(4-Amino-7-methyl-7*H*-pyrrolo[2,3-d]pyrimidin-5-yl)indolin-1-yl)-2-(3-nitrophenyl)ethan-1-one (10c). Prepared using method A to obtain **10c** (73 %) as a yellow solid: m.p. 246–249°C; ^{1}H NMR: δ=8.21 (t, *J* = 3.7 Hz, 1H, H-2''), 8.16–8.14 (m, 2H, H-2, H-4''), 8.11 (d, *J* = 8.3 Hz, 1H, H-7'), 7.77 (d, *J* = 7.8 Hz, 1H, H-6''), 7.65 (t, *J* = 7.8 Hz, 1H, H-5''), 7.32 (d, *J* = 1.0 Hz, 1H, H-4'), 7.25 (s, 1H, H-6), 7.22 (d, *J* = 8.3 Hz, 1H, H-6'), 6.06 (br s, 2H, NH_2-4), 4.27 (t, *J* = 8.4 Hz, 2H, H_2-2'), 4.10 (s, 2H, CH_2), 3.73 (s, 3H, N-Me), 3.25 ppm (t, *J* = 8.4 Hz, 2H, H_2-3'); ^{13}C NMR: δ=168.3 (C=O), 157.1 (C-4), 151.6 (C-2), 150.3 (C-7a), 147.6 (C-3''), 141.7 (C-7'a), 137.6 (C-1''), 136.9 (C-6''), 132.8 (C-3'a), 129.9 (C-5'), 129.5 (C-5''), 127.1 (C-6'), 124.9 (C-4'), 124.6 (C-2''), 124.0 (C-6), 121.5 (C-4''), 116.1 (C-7'), 114.9 (C-5), 99.8 (C-4a), 47.8 (C-2'), 40.9 (CH_2), 30.7 (N-Me), 27.5 ppm (C-3'); MS (APCI): *m/z* (%): 429.2 (100) $[M+H]^+$; HRMS (ESI): *m/z* calcd for $C_{23}H_{21}N_6O_3$: 429.1670 $[M+H]^+$; found: 429.1685; HPLC purity: 98.7 %.

1-(5-(4-Amino-7-methyl-7*H*-pyrrolo[2,3-*d*]pyrimidin-5-yl)indolin-1-yl)-2-(4-nitrophenyl)ethan-1-one (11c). Prepared using method A to obtain **11c** (80 %) as a yellow solid: m.p. 256–258°C; ^{1}H NMR: δ=8.22 (d, *J* = 8.7 Hz, 2H, H-3'', H-5''), 8.14 (s, 1H, H-2), 8.10 (d, *J* = 8.3 Hz, 1H, H-7'), 7.59 (d, *J* = 8.7 Hz, 2H, H-2'', H-6''), 7.32 (br s, 1H, H-4'), 7.24 (s, 1H, H-6), 7.22 (d, *J* = 8.3 Hz, 1H, H-6'), 6.04 (br s, 2H, NH_2-4), 4.25 (t, *J* = 8.4 Hz, 2H, CH_2-2'), 4.08 (s, 2H, CH_2), 3.72 (s, 3H, Me), 3.24 ppm (t, *J* = 8.4 Hz, 2H, CH_2-3'); ^{13}C NMR: δ=168.5 (C=O), 157.6 (C-4), 152.1 (C-2), 150.8 (C-7a), 146.8 (C-4''), 144.0 (C-1''), 142.2 (C-7'a), 133.3

(C-3'a), 131.7 (C-2'', C-6''), 130.4 (C-5'), 127.6 (C-6'), 125.4 (C-4'), 124.5 (C-6), 123.7 (C-3'', C-5''), 116.6 (C-7'), 115.4 (C-5), 100.3 (C-4a), 48.3 (C-2'), 42.0 (CH_2), 31.2 (Me), 28.0 ppm (C-3'); MS (APCI): *m/z* (%): 429.2 (100) $[M+H]^+$; HRMS (ESI): *m/z* calcd for $C_{23}H_{21}N_6O_3$: 429.16697 $[M+H]^+$; found: 429.16895; HPLC purity 98.8 %.

1-(5-(4-Amino-7-methyl-7*H*-pyrrolo[2,3-d]pyrimidin-5-yl)indolin-1-yl)-2-(2-aminophenyl)ethan-1-one (9a). To a suspension of nitrophenylacetamide **9c** (190 mg, 0.44 mmol) in a DMF/acetone/water mixture (3:3:2, 24 mL) was added Zn dust (1.02 g, 15.5 mmol) and ammonium chloride (813 mg, 15.2 mmol). The mixture was stirred at 20 °C for 3 h. The solids were removed by filtration and rinsed with EtOAc (2 x 10 mL). The organic fractions were combined and diluted with EtOAc (50 mL). The organic layer was washed with sat. $NaHCO_3$ (50 mL) and brine (50 mL), dried (Na_2SO_4) and concentrated *in vacuo*. The resulting residue was triturated with EtOAc to obtain the amine **9a** (127 mg, 72 %) as a white solid: m.p. 220–220°C; ^{1}H NMR: δ=8.15–8.13 (m, 2H, H-2, H-7'), 7.29 (s, 1H, H-4'), 7.24–7.21 (m, 2H, H-6, H-6'), 7.01–6.95 (m, 2H, H-4'', H-6''), 6.67 (dd, *J* = 7.9, 0.8 Hz, 1H, H-3''), 6.53 (td, *J* = 7.4, 0.8 Hz, 1H, H-5''), 6.04 (br s, 2H, NH_2-4), 5.05 (s, 2H, NH_2-2''), 4.21 (t, *J* = 8.4 Hz, 2H, H_2-2'), 3.72 (s, 3H, Me), 3.67 (s, 2H, CH_2), 3.20 ppm (t, *J* = 8.4 Hz, 2H, H_2-3'); ^{13}C NMR: δ=169.1 (C=O), 157.1 (C-4), 151.6 (C-2), 150.3 (C-7a), 147.2 (C-2''), 141.9 (C-7'a), 132.8 (C-3'a), 130.3 (C-6''), 129.8 (C-5'), 127.5 (C-4''), 127.1 (C-6'), 124.8 (C-4'), 123.9 (C-6), 118.4 (C-1''), 116.2 (C-7', C-5''), 115.0 (C-3''), 114.9 (C-5), 99.8 (C-4a), 47.9 (C-2'), 39.0 (CH_2), 30.7 (N-Me), 27.5 ppm (C-3'); MS (APCI): *m/z* (%): 399.2 (100) $[M+H]^+$; HRMS (ESI): *m/z* calcd for $C_{23}H_{23}N_6O$: 399.1928 $[M+H]^+$; found: 399.1923; HPLC purity: 99.1 %.

Boc-protected anilines

2-(3-((*tert*-Butoxycarbonyl)amino)phenyl)acetic acid (13). 1M NaOH (4 mL) was added to a solution of 3-aminophenylacetic acid (617 mg, 4.08 mmol) dissolved in 2:1 dioxane/water (12 mL) and di-*tert*-butyl dicarbonate (980 mg, 4.49 mmol) was added. The reaction mixture was stirred at 20 °C for 24 h, neutralised with 2N HCl and diluted with water (50 mL). EtOAc (2 × 50 mL) was added and the organic layer was washed with brine (50 mL), dried and concentrated to an orange gum. The crude residue was purified by column chromatography, eluting with 25 % EtOAc/pet. ether, to give acid **13** (928 mg, 90 %) as a white solid: m.p. 100–102°C; ^{1}H NMR ($CDCl_3$): δ=7.35 (s, 1H), 7.25–7.22 (m, 2H), 6.97–6.94 (m, 1H), 6.60 (br s, 1H), 3.62 (s, 2H), 1.51 (s, 9H); MS (APCI): *m/z* (%): 250.2 (100) $[M-H]^-$.

2-(4-((*tert*-Butoxycarbonyl)amino)phenyl)acetic acid (14).[50] 1M NaOH (5 mL) was added to a solution of 4-aminophenylacetic acid (906 mg, 6.00 mmol) dissolved in 2:1 dioxane/water (15 mL) and then di-*tert*-butyl dicarbonate (1.44 g, 6.59 mmol) was added. The reaction mixture was stirred at 20 °C for 24 h, neutralised with 2N HCl and diluted with water (50 mL). EtOAc (2 × 50 mL) was added and the organic layer was washed with brine (50 mL), dried and concentrated to a white solid. The crude residue was triturated with EtOAc and the carbamate **14** (1.37 g, 91 %) was obtained as a white solid: m.p. 155–157°C; ^{1}H NMR ($CDCl_3$): δ=7.32 (d, *J* = 8.5 Hz, 2H), 7.21 (d, *J* = 8.5 Hz, 2H), 6.48 (br s, 1H), 3.60 (s, 2H), 1.51 (s, 9H); MS (APCI): *m/z* (%): 250.2 (100) $[M-H]^-$.

***tert*-Butyl (3-(2-(5-(4-Amino-7-methyl-7*H*-pyrrolo[2,3-d]pyrimidin-5-yl)indolin-1-yl)-2-oxoethyl)phenyl)carbamate (15).** Prepared using method A and purified by column chromatography (2–3% MeOH/EtOAc) to afford **15** (88 %) as an off-white white solid: m.p. 208–211°C; ^{1}H NMR: δ=9.32 (s, 1H), 8.14–8.12 (m, 2H), 7.45 (s, 1H), 7.32–7.29 (m, 2H), 7.24–7.18 (m, 3H), 6.89 (d, *J* = 7.3 Hz, 1H), 6.03 (br s, 2H), 4.19 (t, *J* = 8.4 Hz, 2H), 3.81 (s, 2H), 3.72 (s, 3H), 3.20 (t, *J* = 8.4 Hz, 2H), 1.47 ppm (s, 9H); MS (APCI): *m/z* (%): 499.2 (100) $[M+H]^+$; HRMS (ESI): *m/z* calcd for $C_{28}H_{31}N_6O_3$: 499.2452 $[M+H]^+$; found: 499.2468.

***tert*-Butyl (4-(2-(5-(4-amino-7-methyl-7*H*-pyrrolo[2,3-d]pyrimidin-5-yl)indolin-1-yl)-2-oxoethyl)phenyl)carbamate (16).** Prepared using method A to obtain **16** (93 %) as a pale brown solid: m.p. 239–242°C; ^{1}H NMR: δ=9.29 (s, 1H), 8.13–8.11 (m, 2H), 7.41–7.39 (m, 2H), 7.29 (s, 1H), 7.24–7.16 (m, 4H), 6.02 (br s, 2H), 4.18 (t, *J* = 8.4 Hz, 2H), 3.77 (s, 2H), 3.72 (s, 3H), 3.19 (t, *J* = 8.4 Hz, 2H), 1.47 ppm (s, 9H); MS (APCI): *m/z* (%): 499.3 (100) $[M+H]^+$; HRMS (ESI): *m/z* calcd for $C_{28}H_{31}N_6O_3$: 499.2452 $[M+H]^+$; found: 499.2470.

Boc-deprotection

1-(5-(4-Amino-7-methyl-7*H*-pyrrolo[2,3-d]pyrimidin-5-yl)indolin-1-yl)-2-(3-aminophenyl)ethan-1-one (10a). TFA (0.5 mL) was added to a stirred solution of *tert*-butyl carbamate **15** (114 mg, 0.23 mmol) in CH_2Cl_2 (10 mL). The reaction was stirred at 20 °C for 4 h and then quenched with sat. $NaHCO_3$ (50 mL). The reaction mixture was extracted with CH_2Cl_2 (50 mL), dried and concentrated *in vacuo*. The resulting residue was triturated with EtOAc to obtain the amine **10a** (88 mg, 96 %) as an off-white solid: m.p. 214–217°C; ^{1}H NMR: δ=8.16–8.14 (m, 2H, H-2, H-7'), 7.28 (s, 1H, H-4'), 7.23–7.21 (m, 2H, H-6, H-6'), 6.96 (t, *J* = 7.7 Hz, 1H, H-5''), 6.51 (s, 1H, H-2''), 6.45–6.43 (m, 2H, H-4'', H-6''), 6.04 (br s, 2H, NH_2-4), 5.04 (s, 2H, NH_2-3''), 4.14 (t, *J* = 8.5 Hz, 2H, H_2-2'), 3.72 (s, 3H, N-Me), 3.67 (s, 2H, CH_2), 3.17 ppm (t, *J* = 8.5 Hz, 2H, H_2-3'); ^{13}C NMR: δ=169.2 (C=O), 157.1 (C-4), 151.6 (C-2), 150.3 (C-7a), 148.8 (C-3''), 141.9 (C-7'a), 135.3 (C-1''), 132.7 (C-3'a), 129.8 (C-5'), 128.9 (C-5''), 127.1 (C-6'), 124.8 (C-4'), 123.9 (C-6), 116.6 (C-6''), 116.2 (C-7'), 114.9 (C-5), 114.3 (C-2''), 112.3 (C-4''), 99.8 (C-4a), 47.9 (C-2'), 42.8 (CH_2), 30.7 (N-Me), 27.5 ppm (C-3'); MS (APCI): *m/z* (%): 399.2 (100) $[M+H]^+$; HRMS (ESI): *m/z* calcd for $C_{23}H_{23}N_6O$: 399.1928 $[M+H]^+$; found: 399.1942; HPLC purity: 97.7 %.

1-(5-(4-Amino-7-methyl-7*H*-pyrrolo[2,3-d]pyrimidin-5-yl)indolin-1-yl)-2-(4-aminophenyl)ethan-1-one (11a). TFA (0.5 mL) was added to a stirred solution of *tert*-butyl carbamate **16** (120 mg, 0.24 mmol) in CH_2Cl_2 (10 mL). The reaction was stirred at 20 °C for 5 h and quenched with sat. $NaHCO_3$ (50 mL). The reaction mixture was extracted with CH_2Cl_2 (40 mL), dried and concentrated *in vacuo*. The resulting residue was triturated with EtOAc to obtain the amine **11** (83 mg, 86 %) as an off-white solid: m.p. 147–150°C; ^{1}H NMR: δ=8.14–8.12 (m, 2H, H-2, H-7'), 7.27 (s, 1H, H-4'), 7.23–7.20 (m, 2H, H-6, H-6'), 6.95 (d, *J* = 8.3 Hz, 2H, H-2'', H-6''), 6.52 (d, *J* = 8.3 Hz, 2H, H-3'', H-5''), 6.04 (br s, 2H, NH_2-4), 4.95 (s, 2H, NH_2-4''), 4.15 (t, *J* = 8.4 Hz, 2H, H_2-2'), 3.72

(s, 3H, N-Me), 3.63 (s, 2H, CH_2), 3.17 ppm (t, *J* = 8.4 Hz, 2H, H_2-3'); ^{13}C NMR: δ=169.8 (C=O), 157.1 (C-4), 151.6 (C-2), 150.3 (C-7a), 147.2 (C-4''), 142.0 (C-7'a), 132.7 (C-3'a), 129.7 (C-5', C-2'', C-6''), 127.1 (C-6'), 124.8 (C-4'), 123.9 (C-6), 121.5 (C-1''), 116.2 (C-7'), 115.0 (C-5), 113.9 (C-3'', C-5''), 99.8 (C-4a), 47.9 (C-2'), 41.6 (CH_2), 30.7 (N-Me), 27.5 ppm (C-3'); MS (APCI): *m/z* (%): 399.2 (100) $[M+H]^+$; HRMS (ESI): *m/z* calcd for $C_{23}H_{23}N_6O$: 399.1928 $[M+H]^+$; found: 399.1942; HPLC purity: 98.5 %.

Preparation of prodrug triggers

5-(Chloromethyl)-1-methyl-2-nitro-1*H*-imidazole (18). MsCl (149 µL, 1.93 mmol) was added to mixture of (1-methyl-2-nitro-1*H*-imidazol-5-yl)methanol (**17**) (253 mg, 1.61 mmol) and DIPEA (337 µL, 1.93 mmol) stirring in THF (5mL). The mixture was stirred at 20 °C for 30 min and diluted with EtOAc (20 mL). The organic layer was washed with 1M HCl (20 mL), dried and concentrated *in vacuo*. The chloride **18** (280 mg, 99%) was obtained as a yellow solid which was used without further purification: m.p. 82 °C (decomp.) (lit. [34] 87–90°C, EtOAc); ^{1}H NMR: δ=7.19 (s, 1H, H-4), 4.63 (s, 2H, CH_2), 4.08 ppm (s, 3H, Me); MS (APCI): *m/z* (%): 176.1 (100) $[M+H]^+$.

(1-Methyl-2-nitro-1*H*-imidazol-5-yl)methyl (4-nitrophenyl) carbonate (19).[51] 4-Nitrophenylchloroformate (311 mg, 1.54 mmol) was added to a stirred suspension of alcohol **17** (220 mg, 1.40 mmol) and DIPEA (294 µL, 1.68 mmol) in THF (5 mL). The reaction mixture was stirred at 20 °C for 16 h. The resulting mixture was diluted with EtOAc (50 mL), washed with water (50 mL) and brine (50 mL), dried and concentrated *in vacuo*. The crude residue was purified by column chromatography, eluting with a gradient (60–70 %) of EtOAc/pet. ether to give the carbonate **19** (113 mg, 25 %) as a white solid: m.p. 160–161°C (lit.[45] m.p. 156.5–157.5 °C); ^{1}H NMR: δ=8.35–8.31 (ddd, *J* = 9.2, 3.3, 2.2 Hz, 2H, H-3', H-5'), 7.61–7.57 (ddd, *J* = 9.2, 3.3, 2.2 Hz, 2H, H-2', H-6'), 7.36 (s, 1H, H-4), 5.46 (s, 2H, CH_2), 3.98 ppm (s, 3H, N-Me); MS (APCI): *m/z* (%): 323.1 (100) $[M+H]^+$.

Ether prodrug synthesis

1-(5-(4-Amino-7-methyl-7*H*-pyrrolo[2,3-d]pyrimidin-5-yl)indolin-1-yl)-2-(2-((1-methyl-2-nitro-1*H*-imidazol-5-yl)methoxy)phenyl)ethan-1-one (6b). Phenol **6a** (80 mg, 0.20 mmol), chloride **18** (39 mg, 0.22 mmol) and KI (37 mg, 0.22 mmol) were suspended in DMF (5 mL). K_2CO_3 (55 mg, 0.40 mmol) was added to the mixture, which was heated at 70 °C for 72 h. The mixture was diluted with EtOAc (50 mL), washed with water (2 × 50 mL), brine (50 mL), dried and concentrated in vacuo. The crude residue was purified by preparative HPLC [gradient (95–40–95 %) ammonium formate pH 3.45/90 % CH_3CN/H_2O]. Solvent was removed and the residue was diluted with EtOAc (50 mL), washed with sat. $NaHCO_3$ (50 mL) and brine (50 mL), dried and concentrated. The resulting residue was triturated with EtOAc to obtain ether **6b** (33 mg, 31 %) as a yellow solid: m.p. 228–230 °C; ^{1}H NMR: δ=8.14 (s, 1H, H-2), 8.03 (d, *J* = 8.3 Hz, 1H, H-7'), 7.33–7.28 (m, 2H, H-4'', H-4'''), 7.26–7.17 (m, 5H, H-6, H-4', H-6', H-3'', H-6''), 6.98 (td, *J* = 7.4, 0.8 Hz, 1H, H-5''), 6.10 (br s, 2H, NH_2), 5.24 (s, 2H, OCH_2), 4.11 (t, *J* = 8.6 Hz, 2H, H_2-2'), 3.79 (s, 3H, NCH_3-1'''), 3.73 (s, 5H, CH_2, NCH_3-7), 3.06 (t, *J* = 8.6 Hz, 2H, H_2-3'); ^{13}C NMR: δ=169.0 (C=O), 157.2 (C-4), 155.5 (C-2''), 151.6 (C-2), 150.3 (C-7a), 145.9 (C-2'''), 141.6 (C-7'a), 133.6 (C-5'''), 132.4 (C-3'a), 131.4 (C-6''), 129.8 (C-5'), 128.5 (C-4'''), 128.1 (C-4''), 127.0 (C-6'), 124.7 (C-4', C-1''), 124.0 (C-6), 121.1 (C-5''), 115.9 (C-7'), 115.0 (C-5), 111.9 (C-3''), 99.8 (C-4a), 59.1 (OCH_2), 48.0 (C-2'), 37.0 ($COCH_2$), 34.2 (NCH_3-1'''), 30.7 (NCH_3-7), 27.3 ppm (C-3'); MS (APCI): *m/z* (%): 539.2 (100) $[M+H]^+$; HRMS (ESI): *m/z* calcd for $C_{28}H_{27}N_8O_4$: 539.2150 $[M+H]^+$; found: 539.2150; HPLC purity 98.7 % (0.32 % effector).

1-(5-(4-Amino-7-methyl-7*H*-pyrrolo[2,3-d]pyrimidin-5-yl)indolin-1-yl)-2-(3-((1-methyl-2-nitro-1*H*-imidazol-5-yl)methoxy)phenyl)ethan-1-one (7b). Phenol **7a** (71.5 mg, 0.18 mmol), chloride **18** (34.6 mg), K_2CO_3 (49.5 mg, 0.36 mmol) and KI (32.7 mg, 0.20 mmol) were stirred in DMF (5 mL) at 20 °C overnight (20 h). The resulting mixture was diluted with EtOAc (20 mL), washed with water (20 mL) and with brine (20 mL), dried and concentrated. The crude residue was purified by preparative HPLC [gradient (95–40–95 %) ammonium formate pH 3.45/90 % CH_3CN/H_2O]. Solvent was removed and the residue was diluted with EtOAc (20 mL), washed with sat. $NaHCO_3$ (20 mL) and with brine (20 mL), dried and concentrated. The ether **7b** (30.4 mg, 32 %) was obtained as a pale yellow solid: m.p. 128–131°C; ^{1}H NMR: δ=8.14–8.11 (m, 2H, H-2, H-7'), 7.35 (s, 1H, H-4'''), 7.31–7.27 (m, 2H, H-4', H-5''), 7.24–7.21 (m, 2H, H-6, H-6'), 7.01–6.94 (m, 3H, H-2'', H-4'', H-6''), 6.04 (br s, 2H, NH_2-4), 5.24 (s, 2H, OCH_2), 4.20 (t, *J* = 8.4 Hz, 2H, H_2-2'), 3.96 (s, 3H, NCH_3-1'''), 3.85 (s, 2H, $COCH_2$), 3.72 (s, 3H, NCH_3-7), 3.21 (t, *J* = 8.4 Hz, 2H, H_2-3'); ^{13}C NMR: δ=168.8 ($COCH_2$), 157.5 (C-3''), 157.1 (C-4), 151.6 (C-2), 150.3 (C-7a), 146.2 (C-2'''), 141.8 (C-7'a), 136.8 (C-1''), 133.6 (C-5'''), 132.8 (C-3''a), 129.8 (C-5'), 129.4 (C-4'), 128.5 (C-4'''), 127.1 (C-6'), 124.9 (C-4'), 124.0 (C-6), 122.7 (C-6''), 116.3 (C-2''), 116.2 (C-7'), 114.9 (C-5), 113.0 (C-4''), 99.9 (C-4a), 59.1 (OCH_2), 48.0 (C-2'), 42.0 ($COCH_2$), 34.3 (NCH_3-1'''), 30.7 (NCH_3-7), 27.5 ppm (C-3'); MS (APCI): *m/z* (%): 539.2 (100) $[M+H]^+$; HRMS (ESI): *m/z* calcd for $C_{28}H_{27}N_8O_4$: 539.2150 $[M+H]^+$; found: 539.2168; HPLC purity: 97.6 % (0.27 % effector).

1-(5-(4-Amino-7-methyl-7*H*-pyrrolo[2,3-d]pyrimidin-5-yl)indolin-1-yl)-2-(4-((1-methyl-2-nitro-1*H*-imidazol-5-yl)methoxy)phenyl)ethan-1-one (8b). Phenol **8a** (99 mg, 0.25 mmol), chloride **18** (44 mg, 0.25 mmol), K_2CO_3 (69 mg, 0.50 mmol) and KI (41 mg, 0.25 mmol) were stirred in DMF (5 mL) at 20 °C overnight. A second equivalent of chloride **18** (44 mg, 0.25 mmol) was added to the mixture and was stirred at 20 °C for 43 h. The resulting mixture was diluted with EtOAc (50 mL), washed with water (50 mL) and then brine (50 mL), dried and concentrated *in vacuo*. The resulting crude residue was purified by column chromatography, eluting in 4 % $MeOH/CH_2Cl_2$. Solvent was removed and the mixture triturated with MeOH, filtered, and dried to give the ether **8b** (38 mg, 28 %) as an orange solid: m.p. 246–249°C (decomp.); ^{1}H NMR: δ=8.14–8.12 (m, 2H, H-2, H-7'), 7.34 (s, 1H, H-4'''), 7.30 (s, 1H, H-4'), 7.27–7.21 (m, 4H, H-6, H-6', H-2'', H-6''), 7.05 (d, *J* = 8.68 Hz, 2H, H-3'', H-5''), 6.04 (br s, 2H, NH_2-4), 5.24 (s, 2H, OCH_2), 4.20 (t, *J* = 8.5 Hz, 2H, H_2-2'), 3.96 (s, 3H, NCH_3-1'''), 3.81 (s, 2H, $COCH_2$), 3.73 (s, 3H, NCH_3-7), 3.21 ppm (t, *J* = 8.5 Hz, 2H, H_2-3'); ^{13}C NMR: δ=169.3 (C=O), 157.2 (C-4), 156.2 (C-4''), 151.6 (C-2), 150.3 (C-7a), 146.2 (C-2'''), 141.9 (C-7'a), 133.7 (C-1''), 132.8 (C-3'a), 130.6 (C-2'', C-6''), 129.8 (C-5'), 128.5 (C-4'''), 128.1 (C-5'''), 127.1 (C-6'), 124.9 (C-4'), 124.0 (C-6), 116.2 (C-7'), 114.9 (C-5, C-3'', C-5''), 99.9 (C-4a), 59.2

(OCH_2), 47.9 (C-2'), 41.2 ($COCH_2$), 34.3 (NCH_3-1'''), 30.7 (NCH_3-7), 27.5 ppm (C-2'); HRMS (ESI): *m/z* calcd for $C_{28}H_{27}N_8O_4$: 539.2150 $[M+H]^+$; found: 539.2175; HPLC purity: 93.9 % (0.03 % effector).

Carbamate prodrug synthesis

(1-Methyl-2-nitro-1*H*-imidazol-5-yl)methyl (2-(2-(5-(4-amino-7-methyl-7*H*-pyrrolo[2,3-d]pyrimidin-5-yl)indolin-1-yl)-2-oxoethyl)phenyl)carbamate (9b). To a stirred solution of amine **9a** (92 mg, 0.23 mmol) in THF (10 mL) was added DIPEA (80 µL, 0.46 mmol), HOBt (39 mg, 0.25 mmol) and 5 Å molecular sieves (82 mg). 4-Nitrophenyl carbonate **19** (82 mg, 0.25 mmol) was added and the mixture allowed to stir at 20 °C for 72 h. The resulting mixture was diluted with EtOAc (50 mL), washed with water (50 mL), brine (50 mL) and concentrated. The crude residue was purified by preparative HPLC [gradient (95–40–95 %) ammonium formate pH 3.45/90 % CH_3CN/H_2O]. Solvent was removed and the residue diluted with EtOAc (20 mL), washed with water (20 mL) and brine (20 mL) sequentially, dried and concentrated *in vacuo*. The carbamate **9b** (60 mg, 46 %) was obtained as a pale orange solid: m.p. 172 (decomp.)°C; ^{1}H NMR: δ=9.26 (s, 1H, NHCOO), 8.28 (s, 1H, H-2), 8.08 (d, *J* = 8.2 Hz, 1H, H-7'), 7.52 (d, *J* = 7.3 Hz, 1H, H-3''), 7.39 (s, 1H, H-6), 7.31–7.26 (m, 4H, H-4', H-4'', H-6'', H-4'''), 7.22 (dd, *J* = 8.2, 1.5 Hz, 1H, H-6'), 7.14 (td, *J* = 7.5, 0.9 Hz, 1H, H-5''), 6.75 (br s, 2H, NH_2), 5.26 (s, 2H, OCH_2), 4.19 (t, *J* = 8.4 Hz, 2H, H_2-2'), 3.91 (s, 3H, NCH_3-1'''), 3.89 (s, 2H, $COCH_2$), 3.77 (s, 3H, NCH_3-7), 3.21 ppm (t, *J* = 8.4 Hz, 2H, H_2-3'); ^{13}C NMR: δ=168.9 (C=O), 163.0 (C-2''), 154.6 (C-4), 153.4 (NHCOO), 149.1 (C-7a), 147.8 (C-2), 146.0 (C-2'''), 142.0 (C-7'a), 136.7 (C-1''), 133.4 (C-5'''), 133.0 (C-3'a), 130.9 (C-6''), 128.9 (C-5'), 128.7 (C-4'''), 127.3 (C-4''), 127.1 (C-6'), 125.3 (C-6), 124.9 (C-4'), 124.8 (C-5''), 124.2 (C-3''), 116.3 (C-7'), 116.2 (C-5), 99.2 (C-4a), 55.3 (OCH_2), 47.9 (C-2'), 38.5 ($COCH_2$), 34.2 (NCH_3-1'''), 31.1 (NCH_3-7), 27.4 ppm (C-3'); MS (APCI): *m/z* (%): 423.1 (100) $[M+H]^+$; HRMS (ESI): *m/z* calcd for $C_{29}H_{28}N_9O_5$: 582.2208 $[M+H]^+$; found: 582.2231; HPLC purity: 99.6 % (0.03 % effector).

(1-Methyl-2-nitro-1*H*-imidazol-5-yl)methyl(3-(2-(5-(4-amino-7-methyl-7*H*-pyrrolo[2,3-d] pyrimidin-5-yl)indolin-1-yl)-2-oxoethyl)phenyl)carbamate (10b). Prepared from **10a** and **19** using the same procedure as for **9b**. Purification by preparative HPLC afforded **10b** (58 %) as an orange solid: m.p. 184°C (decomp.); ^{1}H NMR: δ=9.83 (s, 1H, NHCOO), 8.14–8.11 (m, 2H, H-2, H-7'), 7.42 (s, 1H, H-2''), 7.36 (d, *J* = 8.0 Hz, 1H, H-4''), 7.30–7.21 (m, 5H, H-6, H-4', H-6', H-5'', H-4'''), 6.95 (d, *J* = 7.5 Hz, 1H, H-6''), 6.04 (s, 2H, NH_2-4), 5.28 (s, 2H, OCH_2), 4.19 (t, *J* = 8.4 Hz, 2H, H_2-2'), 3.97 (s, 3H, NCH_3-1'''), 3.83 (s, 2H, $COCH_2$), 3.72 (s, 3H, NCH_3-7), 3.20 ppm (t, *J* = 8.4 Hz, 2H, H_2-3'); ^{13}C NMR: δ=168.9 (C=O), 157.1 (C-4), 152.7 (NHCO), 151.6 (C-2), 150.3 (C-7a), 146.1 (C-2'''), 141.8 (C-7'a), 138.8 (C-3''), 135.7 (C-1''), 133.3 (C-5'''), 132.8 (C-3'a), 129.8 (C-5'), 128.8 (C-5'', C-4'''), 127.1 (C-6'), 124.9 (C-4'), 124.0 (C-6, C-6''), 119.2 (C-2''), 116.6 (C-4''), 116.2 (C-7'), 114.9 (C-5), 99.8 (C-4a), 55.1 (OCH_2), 47.9 (C-2'), 42.3 ($COCH_2$), 34.2 (NCH_3-1'''), 30.7 (NCH_3-7), 27.5 ppm (C-3'); MS (APCI): *m/z* (%): 423.1 (100) $[M+H]^+$; HRMS (ESI): *m/z* calcd for $C_{29}H_{28}N_9O_5$: 582.2208 $[M+H]^+$; found: 582.2214; HPLC purity: 99.8 % (0.01 % effector).

(1-Methyl-2-nitro-1*H*-imidazol-5-yl)methyl (4-(2-(5-(4-amino-7-methyl-7*H*-pyrrolo[2,3-*d*]pyrimidin-5-yl)indolin-1-yl)-2-oxoethyl)phenyl)carbamate (11b). Prepared from **11a** and **19** using the same procedure as for **9b**. Purification by preparative HPLC afforded **11b** (9 %) as an orange solid: m.p. >300°C; ^{1}H NMR: δ=9.82 (s, 1H, NHCOO), 8.13–8.11 (m, 2H, H-2, H-7'), 7.41 (d, *J* = 8.24 Hz, 2H, H-3'', H-5''), 7.31–7.29 (m, 2H, H-4', H-4'''), 7.24–7.21 (m, 4H, H-6, H-6', H-2'', H-6''), 6.04 (br s, 2H, NH_2-4), 5.28 (s, 2H, OCH_2), 4.19 (t, *J* = 8.4 Hz, 2H, H_2-2'), 3.97 (s, 3H, NCH_3-1'''), 3.79 (s, 2H, $COCH_2$), 3.72 (s, 3H, NCH_3-7), 3.20 ppm (t, *J* = 8.4 Hz, 2H, H_2-3'); ^{13}C NMR: δ=169.2 (C=O), 157.1 (C-4), 152.7 (NHCOO), 151.6 (C-2), 150.3 (C-7a), 146.1 (C-2'''), 141.9 (C-7'a), 137.2 (C-4''), 133.4 (C-5'''), 132.8 (C-3'a), 129.8 (C-5', C-2'', C-6''), 129.3 (C-1''), 128.8 (C-4'''), 127.1 (C-6'), 124.8 (C-4'), 124.0 (C-6), 118.3 (C-3'', C-5''), 116.2 (C-7'), 114.9 (C-5), 99.8 (C-4a), 55.1 (OCH_2), 47.9 (C-2'), 41.5 ($COCH_2$), 34.2 (NCH_3-1'''), 30.7 (NCH_3-7), 27.5 ppm (C-3'); MS (APCI): *m/z* (%): 423.1 (100) $[M+H]^+$; HRMS (ESI): *m/z* calcd for $C_{29}H_{28}N_9O_5$: 582.2208 $[M+H]^+$; found: 582.2223; HPLC purity: 97.8 % (0.04 % effector).

Radiolytic reduction

Solutions (10 µM) of the prodrugs in deoxygenated 0.1M sodium formate/5 mM sodium phosphate buffer (pH 7.0), with a final DMSO concentration of 0.1%, were prepared in a Bactron Pd/H_2-scrubbed anaerobic chamber (Sheldon Manufacturing Inc. Cornelius, OR), transferred to HPLC vials and sealed. Solutions were irradiated with 40 Gy (ca 2.5 Gy/min, Eldorado78 ^{60}Cobalt source) and stored at -80 °C until analysis by LC-MS (See below). The chromatograms of the irradiated samples were compared to prodrug and effector samples without radiation (See Figure S2).

Cell culture

HCT116 colorectal carcinoma cells were cultured in alpha minimum essential medium (αMEM, ThermoFisher Scientific, Auckland, New Zealand) supplemented with 5% (v/v) fetal bovine serum (FBS; Moregate Biotech, Hamilton, NZ). Cell line authenticity was confirmed by short tandem repeat analysis and cultures were demonstrated to be mycoplasma negative.

RT-qPCR

Cells (2×10^5) were seeded in 6-well plates (ThermoFisher Scientific) in 1.5 mL αMEM + 5% FBS. An additional 1.5 mL of αMEM + 5% FBS was added containing either compound to achieve a final concentration of 10 µM, or an equivalent volume of DMSO (final concentration of 0.1%). Samples were then cultured in either 20%O_2/5%CO_2/N_2 (oxic) or in 0%O_2/5% CO_2/N_2 (anoxic) conditions (H45 HEPA Hypoxystation; Don Whitley Scientific, West Yorkshire, United Kingdom). After 24 h incubation, the culture medium was aspirated and RNA was extracted using TRIzol reagent (ThermoFisher Scientific), quantified by NanoDrop (ThermoFisher Scientific) and converted to cDNA using a High Capacity cDNA Reverse Transcription Kit (ThermoFisher Scientific). Quantitative PCR was carried out using SYBER Select Master Mix (ThermoFisher Scientific) on a QuantStudio 6 Flex Real-Time PCR instrument. Relative gene expression was

calculated using the comparative CT method (2-ΔΔCT method). Primer sequences were as follows: *DDIT3 (CHOP)* Forward 5'-GGAGCATCAGTCCCCCACTT, Reverse 5'-TGTGGGATTGAGGGTCACATC; *PPP1R15A (GADD34)* Forward 5'-CCCAGAAACCCCTACTCATGATC, Reverse 5'-GCCCAGACAGCCAGGAAAT; HPRT1 Forward 5'-CCAGTCAACAGGGGACATAAA, Reverse 5'-CACAATCAAGACATTCTTTCCAGT.

Western Immunoblotting

Samples were prepared as above, except 1 × 10^6 cells were seeded into 10 cm culture dishes (Corning NY) in 7.5 mL αMEM + 5% FBS and an additional 7.5 mL of αMEM + 5% FBS containing compound/0.1% DMSO added. After 24 h oxic or anoxic incubation, cell monolayers were washed twice using 10 mL of ice-cold PBS and then lysed in 0.5 mL RIPA buffer (50 mM Tris-HCl pH 7.4, 1% IGEPAL® CA-630, 0.25% sodium deoxycholate, 0.1% SDS, 150 mM NaCl, 1 mM EDTA) supplemented with 1 × protease inhibitor (P8340; Sigma-Aldrich, St Louis, MO). Protein lysates were separated on 4–12% Bis-Tris gels (ThermoFisher Scientific). Proteins were then wet transferred onto polyvinylidene fluoride membranes (Merck Millipore, Burlington, MA), blocked for 1 h with 5% non-fat milk in TBS-T and then incubated overnight at 4 °C with primary antibody diluted 1:1000 in blocking buffer. Detection of signal utilised HRP-conjugated secondary antibodies (ThermoFisher Scientific), chemiluminescent reagent (ThermoFisher Scientific) and imaging using a ChemiDoc MP Imaging System (Bio-Rad, Hercules, CA). Primary antibodies were as follows; ATF4 (clone D4B8, Cell Signaling Technology, Danvers, MA), CHOP (clone L63F7, Cell Signaling Technology), β-actin (clone C4, Merck Millipore).

Mass spectrometry methods

Extracellular medium samples (from RT-qPCR plates) were frozen at -80 °C after collection until analysis. Samples were thawed on ice and vortexed vigorously. An aliquot (100 µL) of the sample was added into 200 µL of ice cold methanol, spun at 13000 rpm, 4 °C for 2 minutes. The supernatant was collected and analysed on an Agilent Technologies Single Quadrupole MS 6450b LC-MS interfaced with an Agilent Jet Stream Electrospray Ionization (ESI) source allowing positive or negative ion detection. Mobile phases were (A) 45 mM formate buffer, pH 4.5 and (B) 80 % acetonitrile + 0.01 % formic acid with a Zorbax, C18 3 x 150 mm, 5 µm column running at a flow rate of 0.5 mL/min with an injection volume of 50 µL. Three point calibration curves (10, 3.33, 1.11 µM) were made fresh on the day of analysis.

Acknowledgements

The authors thank Dr Jack Flanagan for helpful discussions and thank Dr Adrian Blaser, Ms Karin Tan, and Mr Sisira Kumara for technical assistance. The authors would like to acknowledge the support of the University of Auckland Faculty Research Development Fund.

Keywords: drug delivery, hypoxia, kinase inhibitor, nitroimidazole, prodrug

References:

[1] M. Koritzinsky, F. Levitin, T. van den Beucken, R. A. Rumantir, N. J. Harding, K. C. Chu, P. C. Boutros, I. Braakman, B. G. Wouters, *J. Cell Biol.* **2013**, *203*, 615–627.

[2] D. E. Feldman, V. Chauhan, A. C. Koong, *Mol. Cancer Res.* **2005**, *3*, 597–605.

[3] D. Ron, P. Walter, *Nat. Rev. Mol. Cell Biol.* **2007**, *8*, 519–529.

[4] M. Wang, R. J. Kaufman, *Nat. Rev. Cancer* **2014**, *14*, 581–597.

[5] J. Han, S. H. Back, J. Hur, Y.H. Lin, R. Gildersleeve, J. Shan, C. L. Yuan, D. Krokowski, S. Wang, M. Hatzoglou, M. S. Kilberg, M. A. Sartor, R. J. Kaufman, *Nat. Cell Biol.* **2013**, *15*, 481–490.

[6] M. Bi, C. Naczki, M. Koritzinsky, D. Fels, J. Blais, N. Hu, H. Harding, I. Novoa, M. Varia, J. Raleigh, D. Scheuner, R. J. Kaufman, J. Bell, D. Ron, B. G. Wouters, C. Koumenis. *EMBO J.* **2005**, *24*, 3470–3481.

[7] D. Cojocari, R. N. Vellanki, B. Sit, D. Uehling, M. Koritzinsky, B. G. Wouters, *Radiother. Oncol.* **2013**, *108*, 541–547.

[8] A. Bertolotti, Y. Zhang, L. M. Hendershot, H. P. Harding, D. Ron, *Nat. Cell. Biol.* **2000**, *2*, 326–332.

[9] M. Carrara, F. Prischi, P. R. Nowak, M. M. Ali, *EMBO J.* **2015**, *34*, 1589–1600.

[10] H. P. Harding, Y. Zhang, H. Zeng, I. Novoa, P. D. Lu, M. Calfon, N. Sadri, Y. Chi, B. Popko, R. Paules, D. F. Stojdl, J. C. Bell, T. Hettmann, J. M. Leiden, D. Ron. *Mol. Cell* **2003**, *11*, 619–633.

[11] J. M. Axten, J. R. Medina, Y. Feng, A. Shu, S. P. Romeril, S. W. Grant, W. H. H. Li, D. A. Heerding, E. Minthorn, T. Mencken, C. Atkins, Q. Liu, S. Rabindran, R. Kumar, X. Hong, A. Goetz, T. Stanley, J. D. Taylor, S. D. Sigethy, G. H. Tomberlin, A. M. Hassell, K. M. Kahler, L. M. Shewchuk, R. T. Gampe, *J. Med. Chem.* **2012**, *55*, 7193–7207.

[12] J. M. Axten, S. P. Romeril, A. Shu, J. Ralph, J. R. Medina, Y. Feng, W. H. H. Li, S. W. Grant, D. A. Heerding, E. Minthorn, T. Mencken, N. Gaul, A. Goetz, T. Stanley, A. M. Hassell, R. T. Gampe, C. Atkins, R. Kumar, *ACS Med. Chem. Lett.* **2013**, *4*, 964–968.

[13] A. L. Smith, K. L. Andrews, H. Beckmann, S. F. Bellon, P. J. Beltran, S. Booker, H. Chen, Y.-A. Chung, N. D. D'Angelo, J. Dao, K. R. Dellamaggiore, P. Jaeckel, R. Kendall, K. Labitzke, A. M. Long, S. Materna-Reichelt, P. Mitchell, M. H. Norman, D. Powers, M. Rose, P. L. Shaffer, M. M. Wu, J. R. Lipford, *J. Med. Chem.* **2015**, *58*, 1426–1441.

[14] C. Atkins, Q. Liu, E. Minthorn, S.-Y. Zhang, D. J. Figueroa, K. Moss, T. B. Stanley, B. Sanders, A. Goetz, N. Gaul, A. E. Choudhry, H. Alsaid, B. M. Jucker, J. M. Axten, R. Kumar, *Cancer Res.* **2013**, *73*, 1993–2002.

[15] H. P. Harding, A. F. Zyryanova, D. Ron. J. Biol. Chem. **2012**, *287*, 44338–44344.

[16] Q. Yu, B. Zhao, J. Gui, K. V. Katlinski, A. Brice, Y. Gao, C. Li, J. A. Kushner, C. Koumenis, J. A. Diehl, S. Y. Fuchs, *Proc. Natl. Acad. Sci. U. S. A.* **2015**, *112*, 15420–15425.

[17] J. D. Blais, C. L. Addison, R. Edge, T. Falls, H. Zhao, K. Wary, C. Koumenis, H. P. Harding, D. Ron, M. Holcik, J. C. Bell, *Mol. Cell. Biol.* **2006**, *26*, 9517–9532.

[18] K. M. Rouschop, L. J. Dubois, T. G. Keulers, T. van den Beucken, P. Lambin, J. Bussink, A. J. van der Kogel, M. Koritzinsky, B. G. Wouters, *Proc. Natl Acad. Sci. USA*, **2013**, *110*, 4622-4627.

[19] H. Mujcic, A. Nagelkerke, K. M. Rouschop, S. Chung, N. Chaudary, P. N. Span, B. Clarke, M. Milosevic, J. Sykes, R. P. Hill, M. Koritzinsky, B. G. Wouters, *Clin. Cancer Res.* **2013**, *19*, 6126–6137.

[20] Y. X. Feng, E. S. Sokol, C. A. Del Vecchio, S. Sanduja, J. H. Claessen, T. A Proia, D. X. Jin, F. Reinhardt, H. L. Ploegh, Q. Wang, P. B. Gupta, *Cancer Discov.* **2014**, *4*, 702–715.

[21] N. Dhani, A. Fyles, D. Hedley, M. Milosevic, *Sem. Nuclear Med.* **2015**, *45*, 110–121.

[22] S. M. Evans, K. L. Du, A. A. Chalian, R. Mick, P. J. Zhang, S. M. Hahn, H. Quon, R. Lustig, G. S. Weinstein, C. J. Koch, *Int. J. Radiat. Oncol. Biol. Phys.* **2007**, *69*, 1024–1031.

[23] P. Vaupel, A. Mayer, *Cancer Metastasis Rev.* **2007**, *26*, 225–239.

[24] S. Chouaib, M.Z. Noman, K. Kosmatopoulos, M.A. Curran, *Oncogene* **2017**, *36*, 439–445.

[25] M. P. Hay, K. O. Hicks, J. Wang, in *Tumor Microenvironment and Cellular Stress* (Eds.: C. Koumenis, E. Hammond, A. Giaccia), Springer New York, New York, NY, 2014, pp. 111–145.

[26] W. R. Wilson, M. P. Hay, *Nat. Rev. Cancer* **2011**, *11*, 393–410.

[27] I. N. Mistry, M. Thomas, E. D. D. Calder, S. J. Conway, E. M. Hammond, *Int. J. Radiat. Oncol. Biol. Phys.* **2017**, *98*, 1183–1196.

[28] R. M. Phillips, *Cancer Chemother. Pharmacol.* **2016**, *77*, 441-457.

[29] A. V. Patterson, D. M. Ferry, S. J. Edmunds, Y. Gu, R. S. Singleton, K. Patel, S. M. Pullen, K. O. Hicks, S. P. Syddall, G. J. Atwell, S. Yang, W. A. Denny, W. R. Wilson, *Clin. Cancer Res.* **2007**, *13*, 3922–3942.

[30] M. P. Hay, K. O. Hicks, W.R. Wilson, in *Comprehensive Medicinal Chemistry III*, Vol. 8, Case Histories in Recent Drug Discovery (Eds.: D. Rotella, S. Chackalamannil, S. Ward), Elsevier, Amsterdam, Netherlands, 2017, pp. 58–94.

[31] K. O. Hicks, B. G. Siim, J. K. Jaiswal, F. B. Pruijn, A. M. Fraser, R. Patel, A. Hogg, H. D. S. Liyanage, M. J. Dorie, J. M. Brown, W. A. Denny, M. P. Hay, W. R. Wilson, *Clin. Cancer Res.* **2010**, *16*, 4946–4956.

[32] J. D. Sun, Q. Liu, J. Wang, D. Ahluwalia, D. Ferraro, Y. Wang, J.-X. Duan, W. S. Ammons, J. G. Curd, M. D. Matteucci, C. P. Hart, *Clin. Cancer Res.* **2012**, *18*, 758–770.

[33] G.-L. Lu, A. Ashoorzadeh, R. F. Anderson, A. V. Patterson, J. B. Smaill, *Tetrahedron* **2013**, *69*, 9130–9138.

[34] L. J. O'Connor, C. Cazares-Körner, J. Saha, C. N. G. Evans, M. R. L. Stratford, E. M. Hammond, S. J. Conway, *Nat. Protoc.* **2016**, *11*, 781–794.

[35] R. Zhu, M.-C. Liu, M.-Z. Luo, P. G. Penketh, R. P. Baumann, K. Shyam, A. C. Sartorelli, *J. Med. Chem.* **2011**, *54*, 7720–7728.

[36] M. P. Hay, G. J. Atwell, W. R. Wilson, S. M. Pullen, W. A. Denny, *J. Med. Chem.* **2003**, *46*, 2456–2466.

[37] M. P. Hay, B. M. Sykes, W. A. Denny, C. J. O'Connor, *J. Chem. Soc., Perkin Trans. 1* **1999**, 2759–2770.

[38] M. P. Hay, B. M. Sykes, W. A. Denny, W. R. Wilson, *Bioorg. Med. Chem. Lett.* **1999**, *9*, 2237–2242.

[39] M. P. Hay, W. R. Wilson, W. A. Denny, *Bioorg. Med. Chem. Lett.* **1999**, *9*, 3417–3422.

[40] M. Tercel, A. E. Lee, A. Hogg, R. F. Anderson, H. H. Lee, B. G. Siim, W. A. Denny, W. R. Wilson, *J. Med. Chem.* **2001**, *44*, 3511–3522.

[41] R. F. Borch, J. Liu, J. P. Schmidt, J. T. Marakovits, C. Joswig, J. J. Gipp, R. T. Mulcahy, *J. Med. Chem.* **2000**, *43*, 2258–2265.

[42] J.-X. Duan, H. Jiao, J. Kaizerman, T. Stanton, J. W. Evans, L. Lan, G. Lorente, M. Banica, D. Jung, J. Wang, H. Ma, X. Li, Z. Yang, R. M. Hoffman, W. S. Ammons, C. P. Hart, M. Matteucci, *J. Med. Chem.* **2008**, *51*, 2412–2420.

[43] S. A. Everett, M. A. Naylor, K. B. Patel, M. R. L. Stratford, P. Wardman, *Bioorg. Med. Chem. Lett.* **1999**, *9*, 1267–1272.

[44] I. Parveen, D. P. Naughton, W. J. D. Whish, M. D. Threadgill, *Bioorg. Med. Chem. Lett.* **1999**, *9*, 2031–2036.

[45] M. P. Hay, R. F. Anderson, D. M. Ferry, W. R. Wilson, W. A. Denny, *J. Med. Chem.* **2003**, *46*, 5533–5545.

[46] M. P. Hay, W. R. Wilson, W. A. Denny, *Bioorg. Med. Chem.* **2005**, *13*, 4043-4055.

[47] L. J. O'Connor, C. Cazares-Korner, J. Saha, C. N. G. Evans, M. R. L. Stratford, E. M. Hammond, S. J. Conway, *Org. Chem. Front.* **2015**, *2*, 1026–1029.

[48] F. W. Hunter, R. J. Young, Z. Shalev, R. N. Vellanki, J. Wang, Y. Gu, N. Joshi, S. Sreebhavan, I. Weinreb, D. P. Goldstein, J. Moffat, T. Ketela, K. R. Brown, M. Koritzinsky, B. Solomon, D. Rischin, W. R. Wilson, B. G. Wouters, *Cancer Res.* **2015**, *75*, 4211–4223.

[49] D. Rojas-Rivera, T. Delvaeye, R. Roelandt, W. Nerinckx, K. Augustyns, P. Vandenabeele, M. J. M. Bertrand, *Cell Death Differentiat.* **2017**, *24*, 1100–1110.

[50] B. Budke, J. H. Kalin, M. Pawlowski, A. S. Zelivianskaia, M. Wu, A. P. Kozikowski, P. P. Connell, *J. Med. Chem.* **2013**, *56*, 254–263.

[51] M. P. Hay, W. R. Wilson, W. A. Denny, *Tetrahedron* **2000**, *56*, 645–657.

10.1002/asia.201801826

Entry for the Table of Contents

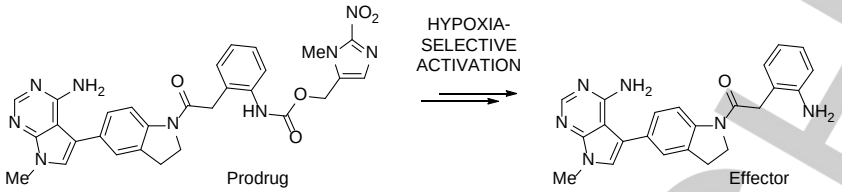

Tumour hypoxia causes endoplasmic reticulum (ER) stress which is moderated through protein kinase R-like ER kinase (PERK) mediated signaling. However, hypoxia also presents a tumour-selective target for prodrug delivery. We designed and prepared hypoxia-activated prodrugs of PERK inhibitors and evaluated their activity as PERK inhibitors, their hypoxia-selective activation and their modulation of PERK signalling in cells.